PCCP

Accepted Manuscript

ROYAL SOCIETY OF CHEMISTRY

www.rsc.org/pccp

Cite this: DOI: 10.1039/c0xx00000x

www.rsc.org/xxxxxx

ARTICLE TYPE

Improving efficiency of inverted polymer solar cells by introducing inorganic dopants

Chunyu Liu,[a] Jinfeng Li,[a] Xinyuan Zhang,[a] Yeyuan He,[a] Zhiqi Li,[b] Hao Li,[b] Wenbin Guo,*[a] Liang Shen [a] and Shengping Ruan*[b]

Received (in XXX, XXX) XthXXXXXXXXX 20XX, Accepted Xth XXXXXXXXX 20XX
DOI: 10.1039/b000000x

Cadmium selenide (CdSe) quantum dots (QDs) utilized as an additive has been incorporated in polymer solar cells (PSCs) composed of poly [N-9”-hepta-decanyl- 2,7- carbazolealt -5,5- (4’,7’- di-2-thienyl-2’,1’,3’-ben-zothiadiazole)] (PCDTBT) and fullerene derivative [6,6]-phenyl-C71-butyric acid methyl ester ($PC_{71}BM$). The power conversion efficiency (PCE) has been achieved by 6.94% for maximum, corresponding to 33% enhancement compared with the control devices. The introduction of CdSe QDs allows not only improving charge transport property but also tuning the energy levels, which leads to a higher short circuit current (J_{sc}) , fill factor (FF), and open-circuit voltage (V_{oc}).

1. Introduction

Polymer solar cells (PSCs) have been widely investigated since 1995 due to their advantages of flexibility, light weight, low-cost and easy process. [1-7] However, due to the narrow absorption band width, the PSCs power conversion efficiency (PCE) is difficultly to be improved, because only part of photons of the solar spectrum can be utilized efficiently, leading to small short-circuit density (J_{sc}). Up to now, the best PCE was reported to be 10.8% with low band gap polymer as electron donor. [8] Compared with the commercial solar cell technology, to get higher PCE is still a challenge for PSCs.

Furthermore, because of the low mobility of polymer semiconductors, there is competition between the sweep-out of the photogenerated carriers by the built-in potential and recombination of the photogenerated carriers within the thin bulk heterojunction (BHJ) film, useful film thicknesses are limited by recombination. [9] Thus, intensive research efforts have been undertaken to enhance light harvesting and improve chare carrier transport property without increasing the film thickness, such as active layer doping, buffer layer doping, tandem and ternary cascade structure, [10-15] especially the ternary cascade solar cells have attracted great interest due to its good performance. [16,17] Some polymers have been reported as the additive to constitute cascade solar cells with P3HT:PCBM blend previously. Two criteria must be fulfilled for the additive: Firstly, energy levels of the additive should own proper offset with respect to donor and acceptor; Secondly, the additive could play both as electron acceptor and transporter, as well as electron donor and transporter. Hence, the highest occupied molecular orbital (HOMO) and lowest unoccupied molecular orbital (LUMO) of additive is required to be intermediate to those donor and acceptor, creating a cascade energy band structure. Quantum dots (QDs) material possesses theoretical potential to improve performance of PSCs because of its quantum effect and unique optical properties, which has attracted a great deal of interest. In addition, the HOMO and LUMO levels of QDs material can be adjusted via controlling its size to adapt for ternary cascade cells. Many inorganic QDs have been used to replace the fullerenes as electron acceptor to fabricate hybrid solar cells, [18-22] which purposed an important approach to enhance the performance of PSCs.

In this paper, we achieved positive effects arising from the addition of CdSe QDs to BHJ polymer solar cells based on a blend of poly [N-9”-hepta-decanyl- 2,7- carbazolealt -5,5- (4’,7’-di-2-thienyl-2’,1’,3’-ben-zothiadiazole)] (PCDTBT) and fullerene derivative [6,6]-phenyl-C71-butyric acid methyl ester ($PC_{71}BM$). In terms of optimizing the performance of PCDTBT:$PC_{71}BM$ photovoltaics cells, Cadmium selenide (CdSe) QDs were blended into solution to form an assembling ternary cascade structure with various weight ratios (wt) and finally enhanced J_{sc}, open-circuit (V_{oc}), and fill factor (FF) simultaneously.

2. Experimental Section

The synthesis of CdSe QDs has been described elsewhere, and the diameter of CdSe QDs is 10-15 nm. [23] The steady-state absorption and emission spectra of CdSe QDs was shown in Figure.1. It can be seen that CdSe QDs have strong ability of absorbing ultraviolet photons and emitting visible photons at the range of 600 nm to 650 nm, which is located in absorption region of PCDTBT:$PC_{71}BM$ blend. All devices in this work were fabricated with the structure of indium tin oxide (ITO)/nano-crystal titanium dioxide (nc-TiO_2)/ PCDTBT:$PC_{71}BM$:CdSe QDs/molybdenum oxide (MoO_3) /

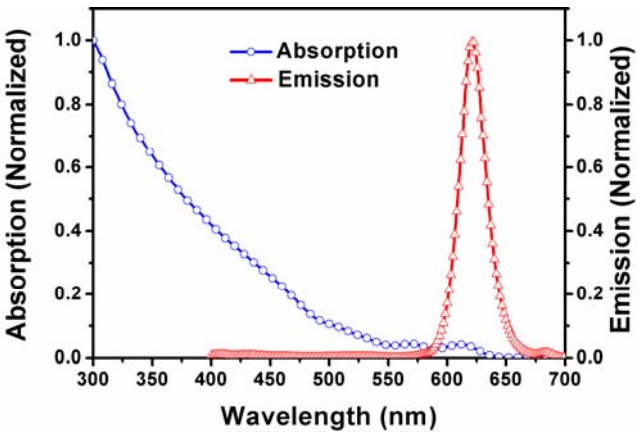

Figure.1 The steady-state absorption and emission spectrum of CdSe QDs under 300 nm to 700 nm.

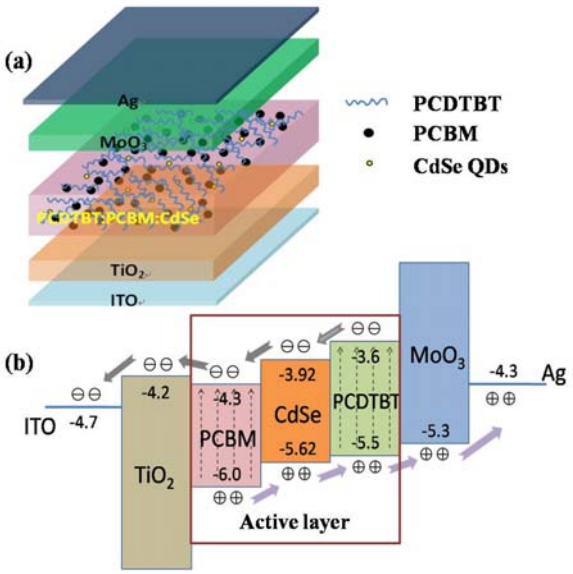

Figure.2 (a) The device structure of the inverted polymer solar cells (b) Scheme of energy levels of the materials involved in the inverted polymer solar cells.

silver (Ag). The schematic structure and energy level of PSCs are shown in Figure.2. The substrates were cleaned by acetone, isopropyl alcohol, and deionized water firstly. Then TiO_2 layer was spin coated onto substrate as an electronic transport layer followed by postannealing at 450°C for 2h in the muffle furnace, and then cooling by nature. The solution containing 7 mg PCDTBT and 28 mg $PC_{71}BM$ in 1mL 1,2-dichlorobenzene (DCB) doping with CdSe QDs was spin coated at 2000 RPM on top of TiO_2 layer in air to be active layer, then conducting a postannealing at 70°C for 20 min in the glove box. The doping ratios of QDs and PCDTBT:$PC_{71}BM$ blend are 1.09wt%, 2.18wt% , 3.27wt%, 4.36wt%, and 6.54wt% respectively. Subsequently, high work function MoO_3 with the ability of enhancing hole collection and Ag anode were thermally evaporated under a base vacuum of 5.0×10^{-4} Pa. All the experiment conditions are selected by foregone experience and

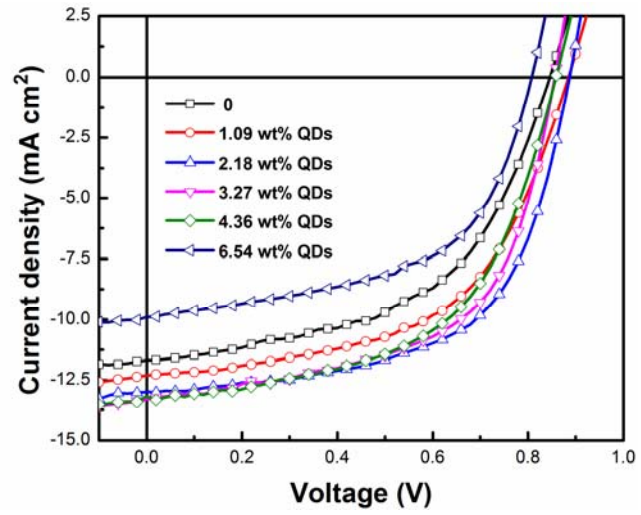

Figure.3 The *J-V* characteristics of devices doping with various amounts of CdSe QDs under AM1.5G illumination with the intensity of 100 mW cm^{-2} in ambient air.

vast experiment progresses. Every active area of the PSCs devices was about 0.064 cm^2.

3. Results and Discussion

The current density-voltage (*J-V*) characteristics of fabricated devices were measured by a Keithley 2400 source measure unit. The photocurrent was measured under Air Mass 1.5 Global (AM 1.5 G) solar illuminations with an irradiation intensity of 100 $mWcm^{-2}$. The light intensity was measured by a photometer (International light, IL1400) and corrected by a standard silicon solar cell. Figure.3 shows the *J-V* characteristics of fabricated devices with different amounts of CdSe QDs doping. Those values of control and doped devices were optimally obtained through several experiment and typical average of 80 devices. The control devices without CdSe QDs exhibit a J_{sc} of 11.69 mA cm^{-2}, voltage of V_{oc} of 0.83 V and FF of 53.2%, leading a PCE of 5.22%. As expected, the performance of devices doped CdSe QDs has been greatly improved, the PCE of cells

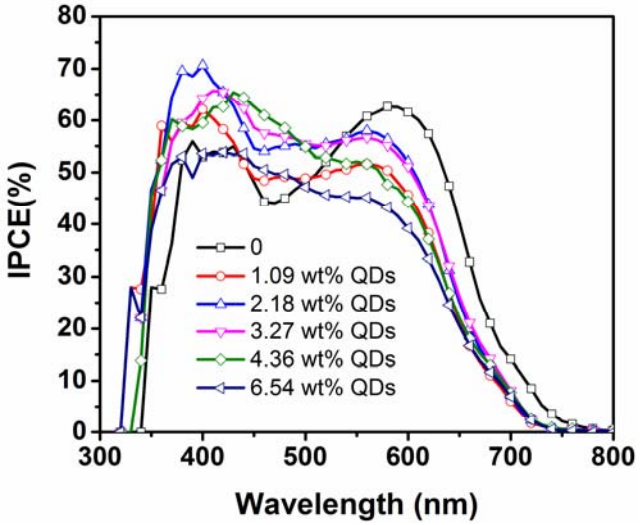

Figure.4 IPCE of inverted polymer solar cells doping with various amounts of CdSe QDs.

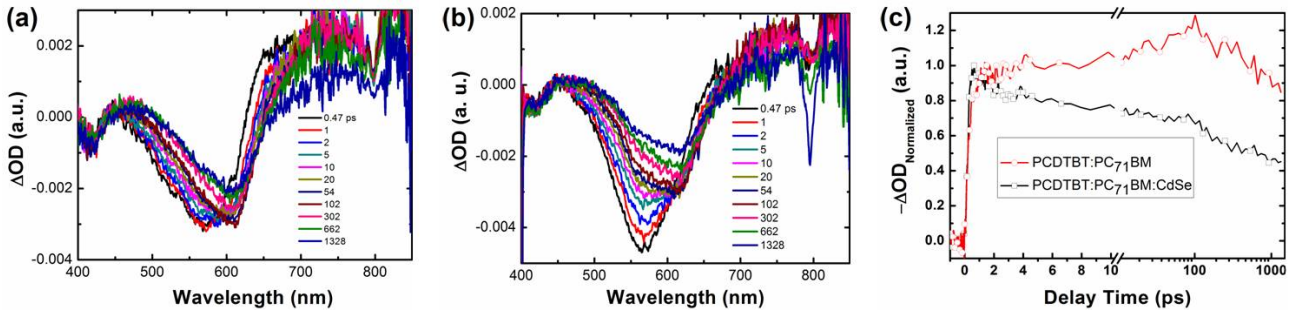

Figure.5 Transient absorption spectra of (a) PCDTBT:$PC_{71}BM$ film and (b) PCDTBT:$PC_{71}BM$:CdSe film, (c) characteristic dynamics for PCDTBT:$PC_{71}BM$ and PCDTBT:$PC_{71}BM$:CdSe films.

made with an optimum ratio of 2.18wt% is 6.94%, with a J_{sc} of 12.98 mA cm^{-2}, V_{oc} of 0.88 V and FF of 60.8%. J_{sc}, V_{oc} and FF are all improved, it is observed that J_{sc} rises from 11.69 mA cm^{-2} to 12.98 mA cm^{-2}, V_{oc} rises from 0.83V to 0.88V and FF rises from 53.2% to 60.8%, which directly leads an enhancement of PCE with 33% higher than control devices. At the same time, the devices doping with ratios of 1.09wt%, 3.27wt% μL, 4.36wt%, and 6.54wt% were also conducted, and some of them demonstrate relatively higher PCE than undoped devices, such as the cells doping with 1.09wt%, 3.27wt% , and 4.36wt% exhibit PCE of 5.98%, 6.47% , and 6.30%, respectively. We can also find that 6.54wt% doping devices produced a negative effect, which shows that excess doping will damage photovoltaic property. The detailed data of all devices performance are summarized in Table 1.

Table 1. Device performance, including open-circuit voltage (V_{oc}), short-circuit current density (J_{sc}), fill factor (FF), and power conversion efficiency (PCE), dependent on the various doping amounts of CdSe QDs.

Doping ratio (wt%)	V_{oc}(V)	J_{sc}(mAcm^{-2})	FF(%)	PCE(%)	Rs (Ω)
0	0.83	11.69	53.2	5.22	253.4
1.09	0.88	12.31	55.2	5.98	248.60
2.18	0.88	12.98	60.8	6.94	148.40
3.27	0.84	13.30	57.9	6.47	161.78
4.36	0.84	13.17	56.9	6.30	217.44
6.54	0.80	9.90	56.2	4.45	179.44

The incident photon-to-current efficiency (IPCE) spectra of all devices are shown in Figure.4. As we can see, the IPCE of control devices shows a maximum of ~62% at 600 nm. When incorporating 2.18wt% QDs, the IPCE of doped cells shows a maximum of ~70% at 400 nm, a little higher than that of the contrast device. It is noticed that the IPCE peak of doping devices occurs an obviously blue shift compared with undoped ones. The IPCE peak movement is derived from the introduction of QDs, because the light absorption of CdSe QDs is focus on the region of 300 nm to 500 nm, which is shown in Figure.1. The higher IPCE band width is larger than the lower IPCE band width for doped devices.

In order to shed the role of CdSe QDs on the performance improvement of doped PSCs, femtosecond transient absorption (TA) spectroscopy was used for PCDTBT:$PC_{71}BM$ and PCDTBT:$PC_{71}BM$:CdSe films at 400 nm excitation (Figure.5). After the pump light excitation, the photoexcited electrons in the excited states could further absorb probe light to high levels or return to ground state by stimulated radiation duo to the disturbance of probe light. And only excited-state absorption has positive signals, the other has negative signals. [24-26] Figure.5 (a) and Figure.5 (b) are the transient absorption spectra of PCDTBT:$PC_{71}BM$ and PCDTBT:$PC_{71}BM$:CdSe film respectively. All these information indicates the condition about the change of photogenerated carrier population in corresponding energy levels. Figure.5 (c) displays the photoexcition signal decay in PCDTBT:$PC_{71}BM$ and PCDTBT:$PC_{71}BM$:CdSe films. The signal response of PCDTBT:$PC_{71}BM$:CdSe exhibits faster decay than that of PCDTBT:$PC_{71}BM$, that is to say the ultrafast photoinduced charge transfer occurred. Figure.5(c) implies that not only do the doped cells exhibit a great number of initial mobile carriers than the undoped cell, but the carriers are also extracted more rapidly, which is consistent with having more balance charge transport, and hence, there is no space charge buildup affecting the internal field as in the case of undoped devices. [27] This process is beneficial for electron transfer across the whole active layer, which may explain J_{sc} and FF improvement of doped devices.

To further confirm the effect of QDs on charge transport properties, we fabricated two kinds of single carrier devices. The hole-only device configuration is ITO/MoO_3/active layer/ MoO_3/Ag, the MoO_3 connected with ITO is electron blocking layer. The electron-only device configuration is ITO/TiO_2/active layer/ BCP/Ag, the BCP is hole blocking layer. The *J-V* characteristics in dark of these two kinds of devices were shown in Figure.6. We observe that J_{sc} of doped devices in Figure.6 (a) have been enhanced irrespective of doping amounts for the hole-only devices, which indicates QDs doping into active layer is

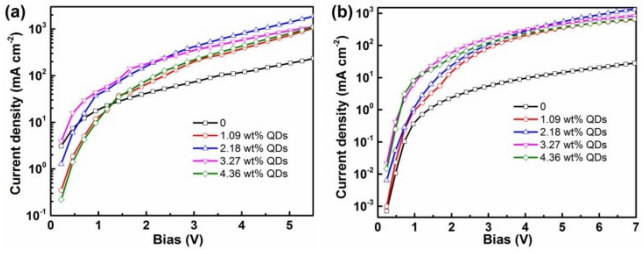

Figure.6 *J-V* characteristics of single charge carrier device in dark (a) hole-only device (b) electron-only device.

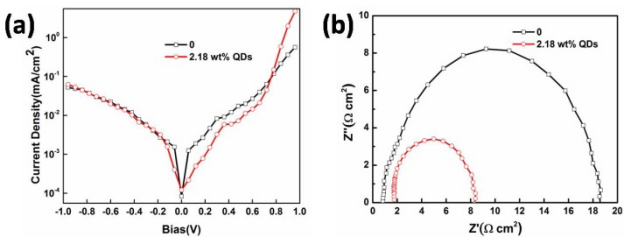

Figure.7 (a) The *J-V* characteristics of devices with various doping amounts of CdSe QDs in dark, (b) the impedance graph of PSCs devices with 2.18wt% CdSe QDs and pristine PCDTBT: $PC_{71}BM$.

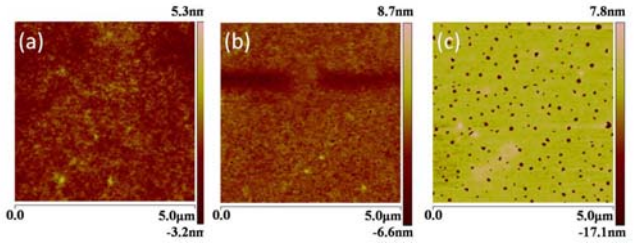

Figure. 8 AFM morphology image of active layer film without and with CdSe QDs, (a) active layer film without CdSe QDs, (b) doping with 1.09wt% QDs, (c) doping with 2.18wt% QDs.

benefit to enhance hole transport properties thus increasing the J_{sc} of doped devices. As the same time, a largest J_{sc} with the doping amount of 2.18wt% was got, which is consistent with the tendency of the photocurrent curves in Figure.3. Figure.6 (b) demonstrates good electron transport capacity of the doped devices, and presents the similar effect as Figure.6 (a), which suggests that both hole and electron transport properties are substantially improved. To investigate the effect of CdSe QDs on the hole and electron transfer properties, we made a realistic evaluation on the apparent charge carrier mobility in the active layer according to *J-V* characteristics of single charge carrier devices. The charge carrier mobility was calculated from the space charge limited current (SCLC) model, which includes field dependence. [28] At a typical applied voltage of 1.0 V, corresponding to an electric field of 10^5 V cm^{-1} across the bulk of a 100 nm device, apparent hole mobilities of 1.46×10^{-3} $cm^2V^{-1}s^{-1}$ and 3.10×10^{-4} $cm^2V^{-1}s^{-1}$ and apparent electron mobility of 4.95×10^{-3} $cm^2V^{-1}s^{-1}$ and 3.10×10^{-5} $cm^2V^{-1}s^{-1}$ have been determined for the 2.18wt% QDs doping and control devices, respectively. That is to say, upon the introducing of CdSe QDs, both the hole and electron mobility increase and a more balanced charge transport in the cells can be achieved. [29] Those are direct evidence that charge transport capacity is largely enhanced by CdSe QDs doping and contributes to improvement of J_{sc}.

Figure. 7 (a) shows the dark *J-V* curves of PSCs with 2.18wt% CdSe doping and without doping. It can be seen that the diffusion current dominated regime is shifted toward higher forward bias in the case of the incorporation of QDs, suggesting that the built-in potential increases when introducing QDs. Impedance spectra was also measured for these two kinds devices, which is shown in Figure.7 (b). The impedance of doped devices is much smaller than undoped devices. At the same times, the series resistance was listed in Table 1. The doped devices possess smaller series resistance, which is conductive to improve the FF of PSCs. V_{oc} of PSCs is limited by the energy difference between the LUMO of acceptor and the HOMO of the donor. But most of PSCs could not reach this fundamental limit under standard testing conditions, the energy loss being typically attributed to charge carrier recombination at the interfaces. [30] From the energy levels in Figure.2(b), it is very clear that the HOMO and LUMO of CdSe QDs are located between the corresponding values of PCDTBT and $PC_{71}BM$, which will create a large energy difference $HOMO_{Donor}$-$LUMO_{Acceptor}$ of PCDTBT:CdSe and CdSe:$PC_{71}BM$ than that of PCDTBT:$PC_{71}BM$ contributing to the increase of V_{oc}. Meanwhile the charge transfer barrier between electron donor (PCDTBT) and electron acceptor ($PC_{71}BM$) can also be reduced when doping CdSe QDs into PCDTBT:$PC_{71}BM$ matrix, and excitons can be dissociated effectively in the junction of PCDTBT:CdSe and CdSe:$PC_{71}BM$. [31-34] The enhanced V_{oc} upon doping of CdSe QDs is a direct consequence of reduced recombination at PCDTBT/$PC_{71}BM$ interfaces. In our previous work, PFDTBT QDs has been introduced into active layer of polymer solar cell, which benefits to charge transport. [35] Compared to PFDTBT QDs, CdSe QDs not only contributes to charge transfer but also helps increase V_{oc}. The doping QDs blocks recombination of electrons in $PC_{71}BM$ with holes in PCDTBT, which leads to a decreased dark current in cascade device, as shown in Figure.7 (a). The reduction in dark current is correlated with the enhancement of V_{oc}. [36,37] Moreover, the ternary cascade structure can accelerate the carrier transfer, resulting in an increased extraction of charge carriers. [38-41] When the doping concentration of QDs is bigger than 2.18wt%, the cells performance will get a reduced trend. The heavy doping may result in bigger roughness compared to that obtained from light doping layer with lower QDs concentration, which leads to that some QDs directly contact with MoO_3/Ag electrode and result in a more serious charge recombination. Figure.8 presents tapping-mode atomic force microscopy (AFM) images (surface area: 5×5 μm^2) of films with 0, 1.09%, and 2.18wt% QDs. Note that the blend films incorporating 1.09wt% and 2.18wt% QDs [Figure.8 (b)and Figure.8 (c)] possessed a rather uneven surface [root-mean-square (RMS) roughness: 12.3 nm and 15.5 nm] relative to that obtained from PCDTBT:$PC_{71}BM$ (RMS roughness: 8.7 nm) (Figure.8 (a)). A rougher active surface layer is more suitable for charge transport to the relative electrodes, thus a great portion of the photogenerated electrons and holes reduced recombination within the blends.

4. Conclusions

In summary, we have demonstrated that simultaneous enhancement of V_{oc}, J_{sc} and FF can be achieved in highly efficient PSCs by simply incorporating CdSe QDs in PCDTBT: $PC_{71}BM$ active layer, resulting in a PCE up to 6.94%. The effects of additive on the improvement of device performance are shown to be twofold: an enhancement of V_{oc} is due to increase the energy difference between acceptor and donor and reduce recombination of electrons and holes, increase of J_{sc} and FF attributes to the improvement of charge carrier transport property. We believe that further improvements in the performance of devices incorporating quantum dots should be possible. The approach here provides a simple and versatile method to optimize PSCs and may set the efficiency of devices towards the goal of 10%.

Acknowledgements

The authors are grateful to National Natural Science Foundation of China (Grant nos. 61275035, 61274068, 61077046), Chinese National Programs for High Technology Research and Development (Grant nos. 2013AA030902), Project of Science and Technology Development Plan of Jilin Province (Grant nos. 20130206075SF), the Opened Fund of the State Key Laboratory on Integrated Optoelectronics (No. IOSKL2012KF03) for the support to the work.

Notes and references

a. State Key Laboratory on Integrated Optoelectronics, Jilin University, 2699 Qianjin Street, Changchun 130012, People's Republic of China
b. College of Electronic Science and Engineering, Jilin University, 2699 Qianjin Street, Changchun 130012, People's Republic of China

1. J. Y. Kim, S. H. Kim, H.-Ho. Lee, K. Lee, W. Ma, X. Gong and A. J. Heeger, Adv. Mater. 2006, **18,** 572.
2. F. C. Krebs, S. A. Gevorgyan and J. Alstrup, J. Mater. Chem. 2009, **19**, 5442.
3. G. Yu, J. Gao, J. C. Hummelen, F. Wudl, and A. J. Heeger, Science 1995, **270**, 1789.
4. C. Edwards, A. Arbabi, G. Popescu and L. L. Goddard, Light Sci. Appl. 2012, **1**, e30.
5. C. Tao, S. Ruan, X. Zhang, G. Xie, L. Shen, X. Kong, W. Dong, C. Liu, W. Chen, Appl. Phys.Lett. 2008, **93**, 193307.
6. H. Zang, Y. Liang, L. Yu, and B. Hu, Adv. Energy Mater. 2011, **1**, 923.
7. H. Y. Chen, J. Hou, S. Zhang, Y. Liang, G. Yang, Y. Yang, L. Yu, Y. Wu and G. Li, Nature Photonics 2009**,** 3**,** 649.
8. Y. H. Liu, J. B. Zhao, Z. K. Li, C. Mu, W. Ma, H. W. Hu, K. Jiang, H. R. Lin, H. Ade, H. Yan, Nature Communications 2014, **5**, 5293.
9. D. H. Wang, D. Y. Kim, K. W. Choi, J. H. Seo, S. H. Im, J. H. Park, O. O. Park, and Alan J. Heeger, Angew. Chem. Int. Ed. 2011, **50**, 5519.
10. R. A. Taylor, T. Otanicar and G. Rosengarten, Light Sci. Appl. 2012, **1**, e34.
11. C. Xiang, W. Koo, F. So, H. Sasabe, J. Kido, Light Sci. Appl. 2013, **2**, e74.
12. H. Q. Wang, M. Batentschuk, A. Osvet, L. Pinna, and C. J. Brabec, Adv. Mater. 2011, **23**, 2675.
13. S. Liu, F. X. Meng, W. F. Xie, Z. H. Zhang, L. Shen, C. Y. Liu, Y. Y. He, W. B. Guo, S. P. Ruan, Appl. Phys. Lett. 2013, **103**, 233303.
14. C. Chen, F. M. Li, Nanoscale Res. Lett. 2013, **8**, 453.
15. F. M. Li, C. Chen, F. R. Tan, G. T. Yue, L. Shen, W. F. Zhang, Nanoscale Res. Lett. 2014, **9**, 240.
16. M. C. Chen, D. J. Liaw, Y. C. Huang, H. Y.Wu, Y. Tai, Sol. Energy Mater. Sol. Cells 2011, **95**, 2621.
17. J. H. Huang, M. Velusamy, K. C. Ho, J. T. Lin, C. W. Chu, J. Mater. Chem. 2010, **20**, 2820.
18. C. F. Guo, T. S. Sun, F. Cao, Q. Liu, Z. F. Ren, Light Sci. Appl. 2014, **3**, e161.
19. L. L. Huang, X. Z. Chen, B. F. Bai, Q. F. Tan, G. F. Jin, T. Zentgraf, S. Zhang, Light Sci. Appl.2013, **2**, e70.
20. X. Chen, B. H. Jia, Y. A. Zhang, M. Gu, Light Sci. Appl. 2013, **2**, e92.
21. Z. Holman, S. Wolf, C. Ballif, Light Sci. Appl. 2013, **2**, e106.
22. Y. Zhou, M. Eck, M. Krüger, Energy Environ. Sci. 2011, **95**, 232.
23. J. Dai, X. Jiang, H. Wang, D. Yan, Appl. Phys. Lett. 2007, **91**, 253503.
24. M. H. Tong, N. E. Coates, D. Moses and Alan. J. Heeger, Physical Review B 2010, **81**, 125210.
25. L. Wang, H. Y. Wang, H. T. Wei, H. Zhang, Q. D. Chen, H. L. Xu, W. Han, B. Yang and H. B. Sun, Adv. Energy Mater. 2014,**1301882**, 1.
26. L. Wang, S.J. Zhu, H. Y. Wang, S. N. Qu, Y. L. Zhang, J. H. Zhang, Q. D. Chen, H. L. Xu, W. Han, B. Yang and H. B. Sun, ACS Nano 2014, **8**, 2541.
27. Y. Zhang, H. Q. Zhou, J. Seifter, L. Ying, A. Mikhailovsky, A. J. Heeger, G. C. Bazan and T. Q. Nguyen,Adv. Mater. 2013, **25**,7038.
28. C. Goh, R. J. Kline, M. D. Mcgehee, E. N. Kadnikova and J. M. J. Frechet, Appl. Phys. Lett. 2005, 86,122110.
29. J. T. Shieh, C. H. Liu, H. F. Meng, S. R. Tseng, Y. C. Chao, and S. F. Horng, J. Appl. Phys. 2010, **107**, 084503.
30. K. Cnops, B. P. Rand, D. Cheyns, and P. Heremans, Appl. Phys. Lett. 2012,**101**, 143301.
31. Y. H. Su, Y.F. Ke, S. L. Cai, Q.Y. Yao, Light Sci. Appl. 2012, **1**, e14.
32. D. Lepage, A. Jimenez, J. Beauvais, J. J. Dubowski, Light Sci. Appl. 2012, **1**, e28.
33. B.C. Thompson, J.M.J. Frechet, Angew. Chem. Int. Ed. 2008, **47**, 58.
34. C.B. Murray, C.R. Kagan, M.G. Bawendi, Science 1995,**270**, 1335.
35. C. Y. Liu, W. B. Guo, H. M. Jiang, L. Shen, S. P. Ruan, D. W. Yan, Organic Electronics, 2014,**15**, 2632.
36. K. Vandewal, K. Tvingstedt, A. Gadisa, O. Inganas, and J. V. Manca, Phys. Rev. B 2010, 81, 125204.
37. N. C. Giebink, G. P. Wiederrecht, M. R. Wasielewski, and S. R. Forrest, Phys. Rev. B 2010, 82, 155305.
38. E. D. Kosten, J. H. Atwater, J. Parsons, A. Polman, H. A. Atwater, Light Sci. Appl. 2013, **2**, e45.
39. L. M. Kristin, I. M. Elizabeth, P. R. Barry, R. F. Stephen, and M. E. Thompson, J. Am. Chem. Soc. 2006, **128**, 8108.
40. M. Y. Jo, S. J. Park, T. Park, Y. S. Wonc, J. H. Kim, Organic Electronics 2012, **13**, 2185.
41. C. J. Brabec, A. Cravino, D. Meissner, N. S. Sariciftci, T. Fromherz, M. T. Rispens, L. Sanchez, and J. C. Hummelen, Adv. Funct. Mater. 2001, **11**, 374.